Scientific paper

Selective Colorimetric Detection of Mn^{2+} and Cr^{2+} Ions using Silver Nanoparticles Modified with Sodium Dodecyl Sulfonate and β-Cyclodextrin

Maryam Akhondi[1,*] and Effat Jamalizadeh[2]

[1] *Department of Chemistry, University of Shahid Bahonar , Kerman, Iran.*

[2] *Department of Chemistry, University of Shahid Bahonar , Kerman, Iran.*

* *Corresponding author: E-mail: m.akhondi67@gmail.com*

Received: 09-07-2019

Abstract

The present study was conducted to determine manganese (Mn^{2+}) and chromium (Cr^{2+}) ions in aqueous systems with a simple, rapid, sensitive, selective and cost-effective colorimetric approach. Sodium dodecyl sulfonate (SDS) and β-cyclodextrin (CD) were used as both stabilizer and surface functionalizing agents for the synthesis of silver nanoparticles (AgNPs). Synthesized AgNPs were characterized by FT-IR spectroscopy, UV-visible spectroscopy, scanning electron microscopy (SEM), transmission electron microscopy (TEM), X-ray diffraction (XRD) and dynamic light scattering (DLS) techniques. The effect of pH on the stability of nanoparticles was investigated. SDS modified silver nanoparticles (SDS-AgNPs) and SDS with **β**-cyclodextrin modified silver nanoparticles (SDS-CD-AgNPs) demonstrated sensitive and selective colorimetric detection of Mn^{2+} and Cr^{2+} ions at ppm level, respectively. The prepared SDS-AgNPs and SDS-CD-AgNPs solution showed a color change visible to the naked eye from yellow to orange upon adding Mn^{2+} and Cr^{2+} ions, respectively; however, other metal ions did not induce such a change. In addition, the results of SEM TEM and DLS" for both sensors showed the aggregation of nanoparticles after adding Mn^{2+} or Cr^{2+}. Overall, the results of this study show the successful synthesis of AgNPs, SDS-AgNPs, and SDS-CD-AgNPs as simple, rapid, sensitive, selective colorimetric sensors with high potential for rapid and on-site detection of Mn^{2+}.

Keywords: Silver nanoparticles; Sodium dodecyl sulfonate; β-cyclodextrin; Colorimetric sensor

1. Introduction

Manganese (Mn) and Chromium (Cr) are essential trace elements for many life processes of the human body such as enzyme activity, bone growth, and fat metabolism.[1,2] However, excessive levels of these elements in biological activities can be toxic for health and may lead to fatal diseases.[3,4] Essential quality standards for Mn (0.05 mg/L) and Cr (0.1 mg/L) have been adopted at the EU level.[5,6] Therefore, the determination of these ions has become inevitable for remedial processes. In this regard, many efforts have been done to detect Mn and Cr ions with high selectivity and sensitivity.

Conventional methods for detecting metal ions are mostly spectroscopy-based techniques such as fluorescent probes,[7,8] atomic absorption,[9,10] surface-enhanced Raman spectroscopy,[11] inductively coupled plasma atomic emission,[12] and inductively coupled plasma mass spectroscopies.[13–15] However, some of these methods are not widely used due to high cost, multi-step sample Pretreatments, and time-intensiveness.[16,17] The attempts to overcome these limitations led to the development of alternative colorimetric sensors. Several colorimetric assays for detecting metal ions in aqueous solutions based on the use of sensitive chromophores or fluorophores,[18] polymers,[19,20] oligonucleotides,[21] DNA,[22,23] and metal nanoparticles[24,25] have been developed. These assays have advantages such as high sensitivity, simplicity, speed and ease of use without the need of any special apparatus.[26] Nanostructured materials have extensive applications in biosensors and ecosensors, especially for detecting metal ions.[27–32] Noble metal nanoparticles, especially gold and AgNPs, have attracted considerable attention in preparing metal ion sensors because of their size and morphology dependent optical properties, strong surface plasmon resonance properties, high extinction coefficient at the visible region, highly stable dispersions, good biocompatibility and chemical inert-

ness.[33,34] Notably, AgNPs have attracted much attention because of lower prices and higher extinction coefficients than those of gold nanoparticles.[16,35,36] The performance of these sensors is based on the surface plasmon resonance (SPR)-induced color variance of nanoparticles, as a result of signal-analyte interaction.[37–40]

Nanoparticles surface functionalization affects the interaction between nanoparticles and metal ions,[38,41] which is critical in the development of noble nanoparticles as a colorimetric sensor for metal ions. For example, among the works conducted in this regard, one can name Ag nanoparticles surface functionalization by octamethoxy resorcin[4]arene tetrahydrazide as a reducing and stabilizing agent for colorimetric detection of cadmium,[42] synthesized AgNPs by cysteic acid as a capping agent for detection of manganese ions,[17] Glutathione-stabilized AgNPs as a colorimetric sensor for nickel ions,[43] thiodisuccinic acid-functionalized AgNPs as a sensor for lead ions,[38] β-cyclodextrin-functionalized AgNPs for detection of mercury and sulfide ions,[44] glutathione-modified AgNPs as a sensor for cobalt ions,[45] dopamine-AgNPs as a sensor for copper ions,[46] AgNPs without any surface modification as a sensor for copper ions,[47] and N-acetyl-L-cysteine-stabilized AgNPs for detection of iron ions.[48]

The purpose of this study is to develop a simple, rapid, efficient and cost-effective method for the determination of some metal ions by functionalized AgNPs. Two new AgNPs based colorimetric sensors were prepared with SDS and SDS-CD as the stabilizing agents without further modification and investigated as colorimetric sensors for Mn^{2+} and Cr^{2+} ions, respectively. There are many published works on colorimetric detection of Mn^{2+} ion based on functionalized AgNPs system; e.g., Pyrophosphate capped AgNPs ($Na_4P_2O_7$),[49] Sodium pyrophosphate (Na4P2O7) and hydroxy propyl methyl cellulose-stabilized AgNPs,[50] 5-sulfoanthranilic acid dithiocarbamate-stabilized AgNPs,[51] L-tyrosine stabilized AgNPs,[52] l-arginine-stabilized AgNPs[16] and alginate-stabilized AgNPs.[53] Although several efforts have been devoted to the development of colorimetric detection of both Cr^{3+} and Cr^{6+} cations,[54–57] based on the functionalized AgNPs system, the detection of Cr^{2+} species has been overlooked. To the best of authors' knowledge, only, Rull-Barrull et al. reported a selective rhodamine-based chemosensor for colorimetric and fluorimetric detection of Cr^{2+} under aqueous conditions.[58]

Herein, the SDS was chosen as a candidate for modifying the AgNPs to design a selective and sensitive colorimetric sensor for detecting Mn^{2+} in the wide range pH (3–13) with a suitable response rate. Also, SDS and CD were chosen to modify the AgNPs to design a selective and sensitive colorimetric sensor for detecting Cr^{2+} in a wide range of pH (i.e., 3–13) with a suitable response rate. Consequently, simple, rapid colorimetric assays for detecting Mn^{2+} and Cr^{2+} were established. These detection methods showed successful detection under various pH conditions. The colorimetric detection mechanism of two sensors, which is based on the accumulation of AgNPs, is illustrated in Figure 1.

2. Experimental

2. 1. Materials

Silver nitrate ($AgNO_3$ ≥ 99%) and β-cyclodextrin (CD ≥ 97%), sodium borohydride ($NaBH_4$, 98%), Hydrochloric acid (HCl, 37%), sodium hydroxide (NaOH, 97%), and Sodium dodecyl sulfonate (SDS ≥ 99.0%) were purchased from Sigma-Aldrich.

2. 2. Instrumentation

UV-vis spectra were recorded on a spectrophotometer (Varian, Cary50), using a 1 cm of quartz cell. Scanning

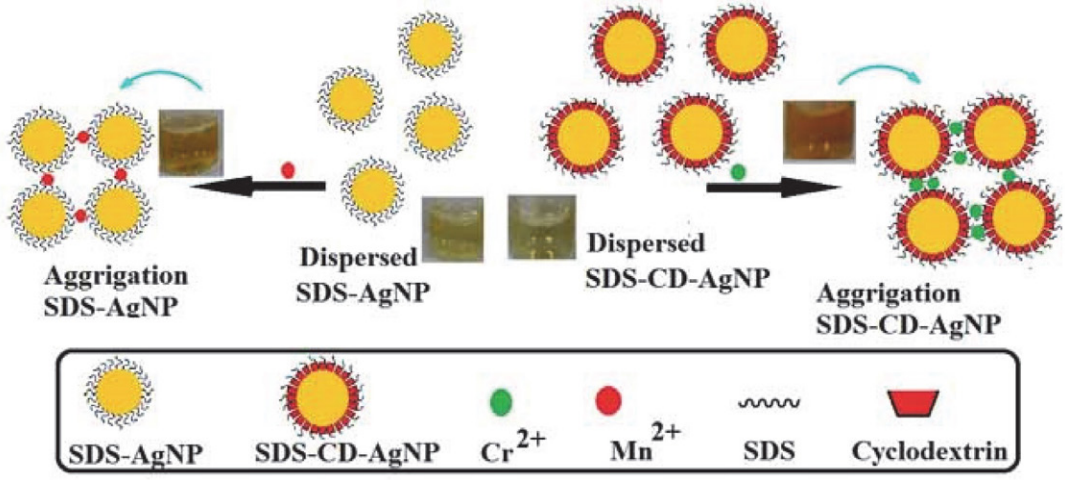

Figure 1. Schematic illustration of detecting mechanism of Mn^{2+} and Cr^{2+} ions based on the aggregation of SDS-AgNPs and SDS-CD-AgNPs, respectively

electron microscopy (SEM) images were obtained using a field-emission scanning electron microscope (KYKT, model EM-3200). Transmission Electron Microscope (TEM) images were recorded from JEOL 2100F TEM. XRD patterns were obtained in reflection mode using a powder X-ray diffractometer (X′ Pert Pro MPD Philips X-ray diffractometer, Ni-filtered Cu-Kα radiation, λ = 0.154 nm). The FT-IR spectra were recorded using the FT-IR spectrometer (Brucker, model Tensor 27) in the region 4,000–400 cm^{-1} using KBr pellets. To determine the mean hydrodynamic diameter (d_H) of the AgNPs in aqueous solution, dynamic light scattering (DLS) investigations were performed without filtering AgNPs solutions at 25 °C using the new non-invasive back-scatter (NIBS) technology by a 1-cm quartz cell. The pH measurements were performed using a pH-meter (METROHM, Model 713).

2. 3. Synthesis of AgNPs

AgNPs were prepared by reducing $AgNO_3$ with $NaBH_4$ in the presence of SDS or mixture of CD and SDS as stabilizing agents. Briefly, 0.1 g of the stabilizing agent was dissolved in 50 ml deionized water. Then, 1.0 mL of $AgNO_3$ aqueous solution (0.001M) was slowly added into the above solution under vigorous stirring for 30 min. Finally, 0.001 g $NaBH_4$ was added into the solution, which caused the color change from yellow to orange.

2. 4. pH-Dependent Stability Study of AgNPs

There are several important factors that affect the stability of the AgNPs.[59] In this section, we will investigate the effect of pH on the stability of AgNPs by monitoring the color variation and UV-vis intensity changes of the AgNPs solution upon the addition of HCl or NaOH solution (0.1 M). In order to study the effect of pH on the stability of AgNPs, the absorption spectra were recorded after 30 min of mixing.

2. 5. Cation-Sensing Studies

The AgNPs sensor behavior in a solution containing various metal ions such as Na^+, K^+, Mg^{2+}, Ca^{2+}, Al^{3+}, As^{3+}, Co^{2+}, Cu^{2+}, Ni^{2+}, Zn^{2+}, Cd^{2+}, Fe^{2+}, Hg^{2+}, Mn^{2+}, and Cr^{2+} ions was studied by recording the UV-vis absorption spectra upon their addition. Thus, 1 ml of each ion solution (10 μM) was added into 1 ml of the freshly prepared AgNPs solution.

For all samples, after 2 min of mixing, some photographs were taken using a digital camera under daytime light and absorption spectra were recorded using a spectrophotometer. The limit of detection (LOD) and limit of quantitation (LOQ) were determined from the standard deviation of the slope of the calibration curve using the following expressions: LOD = 3.3 σ_a /b and LOQ = 10 σ_a /b; where σ_a is the standard deviation of the blank signals and b is the slope of the calibration curve.

To investigate anti-interferential capability of SDS-AgNPs sensors, a mixture of each ion solution (Na^+, K^+, Mg^{2+}, Ca^{2+}, Al^{3+}, As^{3+}, Co^{2+}, Cu^{2+}, Ni^{2+}, Zn^{2+}, Cd^{2+}, Fe^{2+}, Hg^{2+}, and Cr^{2+}) with Mn^{2+} ions was prepared by adding 1 ml of each ion solution (10 μM) into 1 ml 10 μM Mn^{2+} ion solution. Afterward, 1 ml of each solution was mixed with 1 mL SDS-AgNPs solution. This procces was repeated for the SDS-CD-AgNPs with a mixture of each ion solution (Na^+, K^+, Mg^{2+}, Ca^{2+}, Al^{3+}, As^{3+}, Cr^{2+}, Co^{2+}, Cu^{2+}, Ni^{2+}, Zn^{2+}, Cd^{2+}, Fe^{2+}, Hg^{2+}, and Mn^{2+}) with Cr^{2+} ions.

3. Results and Discussion

3. 1. Characterization of Silver Nanoparticles

The synthesized AgNPs were characterized by UV-visible spectroscopy, FT-IR spectroscopy, SEM, TEM, TEM, XRD and DLS techniques. AgNPs absorption spectra in the UV-visible region show a specific absorbance band due to the excitation mode of their surface plasmons by incident light.[60] Based on Mie's theory, spherical nanoparticles have only one SPR band depending on their size.[61,62] Thus, the UV spectrum was used to confirm the synthesis of AgNPs (Figure S1).[61,62] The UV-Visible spectrum shows an absorption maximum that appears at 410 and 400 nm for SDS-AgNPs and SDS-CD-AgNPs, respectively. These values are in good agreement with the literature values for AgNPs.[60] The difference in UV-vis absorption spectra between the SDS-AgNPs and SDS-CD-AgNPs spectrums is due to the variation in the size distribution of the AgNPs as confirmed using SEM and TEM (Figures S2 and 2). The results of SEM and TEM images show that both nanoparticles are polygonal. But, compering these nanoparticles show that SDS-AgNPs have a smaller size with a narrower size distribution than SDS-CD-AgNPs. Based on the TEM results, the average diameter of SDS-AgNPs and SDS-CD-AgNPs are 8 nm and 15 nm, respectively. According to the lectures, using the same reduction reagent, nanoparticle size can be varied by changing the synthesis conditions.[63,64] Probably, the size difference is due to the different rates of diffusion of silver ions into the seed of SDS-AgNPs and SDS-CD-AgNPs. According to previous studies, it is very likely that for both types of nanoparticles (i.e., SDS-AgNPs and SDS-CD-AgNPs), the anionic SDS was adsorbed on the surface of nanoparticles through hydrophobic bonding with a tail surface/headwater orientation. Furthermore, in the presence of cyclodextrin, the hydrophobic carbon chain of SDS was wrapped into the CD cavity-forming host-guest molecules complex.[65] Based on these results for the SDS-CD-AgNPs, the AgNPs were capped by the host-guest inclusion of SDS-CD. And it can be stated that the diffusion of silver ions into the primary seed coated with SDS is more difficult than penetration of silver ions into the primary seed coated with SDS-CD. As a result, the size of SDS-AgNPs is smaller than the size of SDS-CD-AgNPs. In addition, based on the TEM results

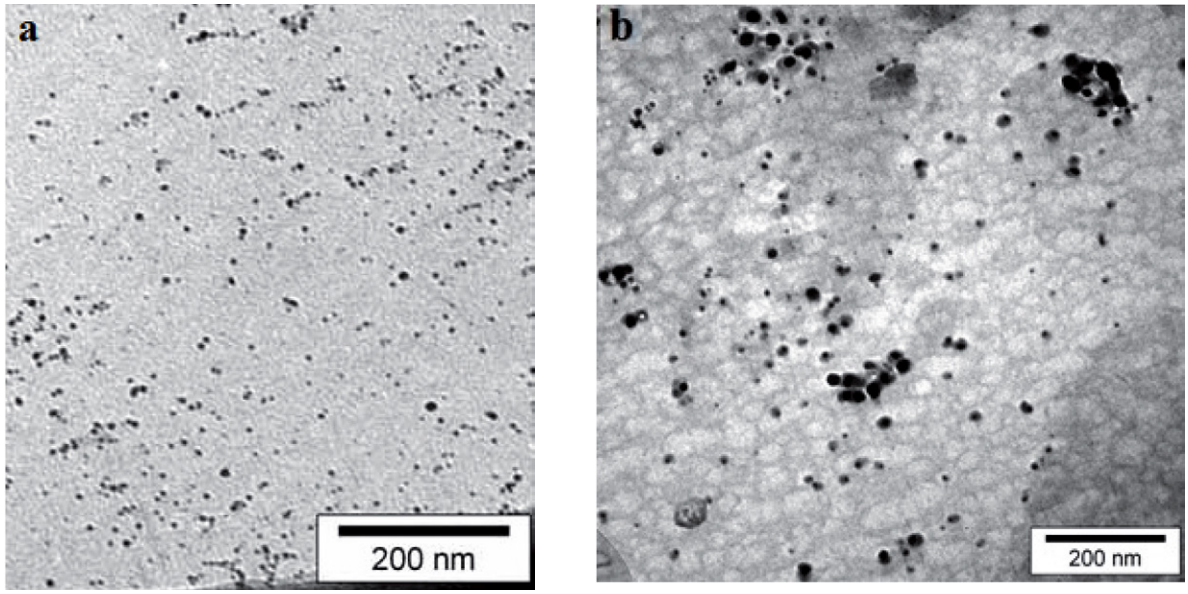

Figure 2. TEM images of the synthesized AgNPs: (a) SDS-AgNPs and (b) SDS-CD-AgNPs.

SDS-CD-AgNPs are more agglomerate than SDS-AgNps. According to the pka values, the SDS surface groups are more deprotonated than the CD groups at neutral pH, consequently, more electrostatic repulsions between the negatively charged groups of SDS-AgNPs, leading to more dispersion of SDS-AgNPs than SDS-CD-AgNPs.[66] In addition, the binding affinity (hydrogen and hydrophobic interactions) between cyclodextrin molecules on the surface of AgNPs leads to some agglomeration of SDS-CD-AgNPs. These agglomeration structures for SDS-CD-AgNPs can be seen in the TEM image.

The effective diameter of the AgNPs in the aqueous solution (pH = 7) was measured by DLS (Figure S3). Unlike the results of TEM, the hydrodynamic diameter of SDS-CD-AgNPs was significantly larger than the hydrodynamic diameter in DLS analysis. Indeed, this analysis shows how a particle diffuses within a fluid while TEM just shows the shape and size of AgNPs.[67]

The FTIR spectra of the SDS-AgNPs and SDS-CD-AgNPs are also recorded to identify the functional groups of the SDS and CD involved in the synthesis of the AgNPs. According to the FTIR spectrums in Figures 3a and 3b, the sharp peaks belonging to the SDS and CD were observed in the spectrum of the AgNPs. In Figure 3a, the FTIR spectra of the SDS-AgNPs and SDS-CD-AgNPs show the peaks at 2943, 2915, 2848, and 1465 cm^{-1} corresponding to the CH_2 stretching and bending modes, the 1220 cm^{-1} peak corresponding to skeletal vibration involving the bridge S–O stretch, and the 1075 cm^{-1} peak corresponding to C–C band stretching of SDS. Also, the peaks at 827 and 579 cm^{-1} correspond to asymmetric C–H bending of the CH_2 group of SDS.[68] The FTIR results are in good agreement with the values reported in literature for SDS. In addition, the spectra of SDS-CD-AgNPs in Figure 3b shows such peaks at 3400 cm^{-1}, 2930 cm^{-1}, and 1155 cm^{-1} corresponding to O–H, C–H, C–O–C bands of CD, respectively; which are in good agreement with the literature values.[69] These results indicate the presence of β-cyclodextrin and SDS as a capping agent of AgNPs.

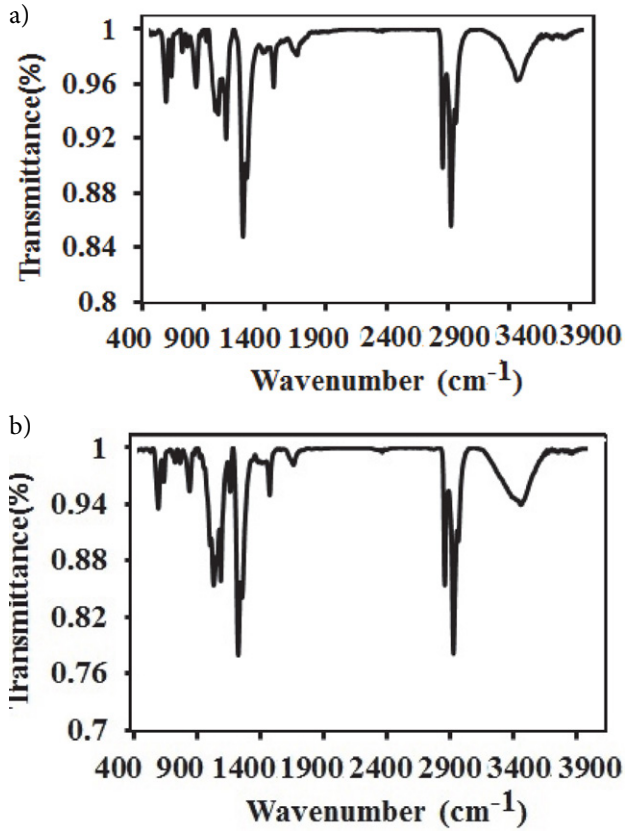

Figure 3 FTIR spectrum of the synthesized AgNPs (a) SDS-AgNP (b) SDS-CD-AgNP.

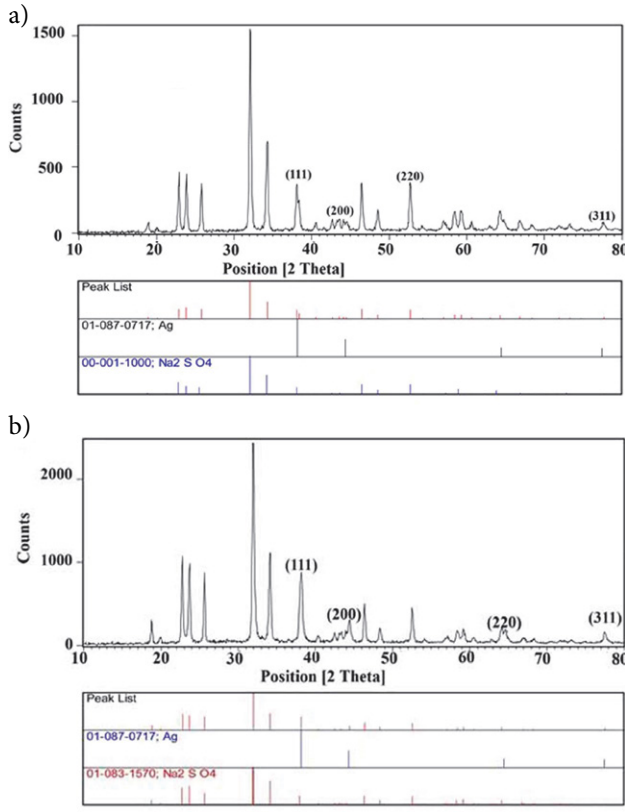

Figure 4. The XRD pattern of (a) SDS-AgNPs and (b) SDS-CD-AgNPs.

Figure 4 shows the XRD spectra of the SDS-AgNPs and SDS-CD-AgNPs after calcination at 500 °C. The XRD pattern of SDS-AgNPs is shown in Figure 4a. The prominent diffraction peaks at 2θ = 38.19°, 44.49°, 64.26° and 77.64° are indexed to the (111), (200), (220), and (311) crystalline planes, respectively. All diffraction peaks indicated that the AgNPs possess a face-centered-cubic (fcc) structure (JCPDS card number 01-087-0717).[70,71] Similarly, the XRD pattern of SDS-CD-AgNPs shows well defined peaks at 2θ = 38.19°, 44.43°, 64.09° and 77.48° are due to the (111), (200), (220), and (311) crystal planes in accordance with a fcc structure of AgNPs (JCPDS card number 01-087-0717).[70, 71]

Moreover, the spectrums of AgNPs contain the XRD characteristic peaks of Na_2SO_4 that corresponded well with those of the standard spectrum. As reported in the literature,[72] SDS undergoes hydrolysis to yield dodecanol and sodium hydrogen sulfate when heated and then it is converted to Na_2SO_4.

3. 2. pH-Dependent Stability Study of AgNPs

As the pH of the solution may influence the surface charge and aggregation of NPs, the pH-dependent stability of SDS-AgNps and SDS-CD-AgNps were studied by UV-visible absorption measurements at the pH range of 1–13 Figure S4. The results show that the SDS-AgNPs are stable in the pH range of 3–11. However, according to

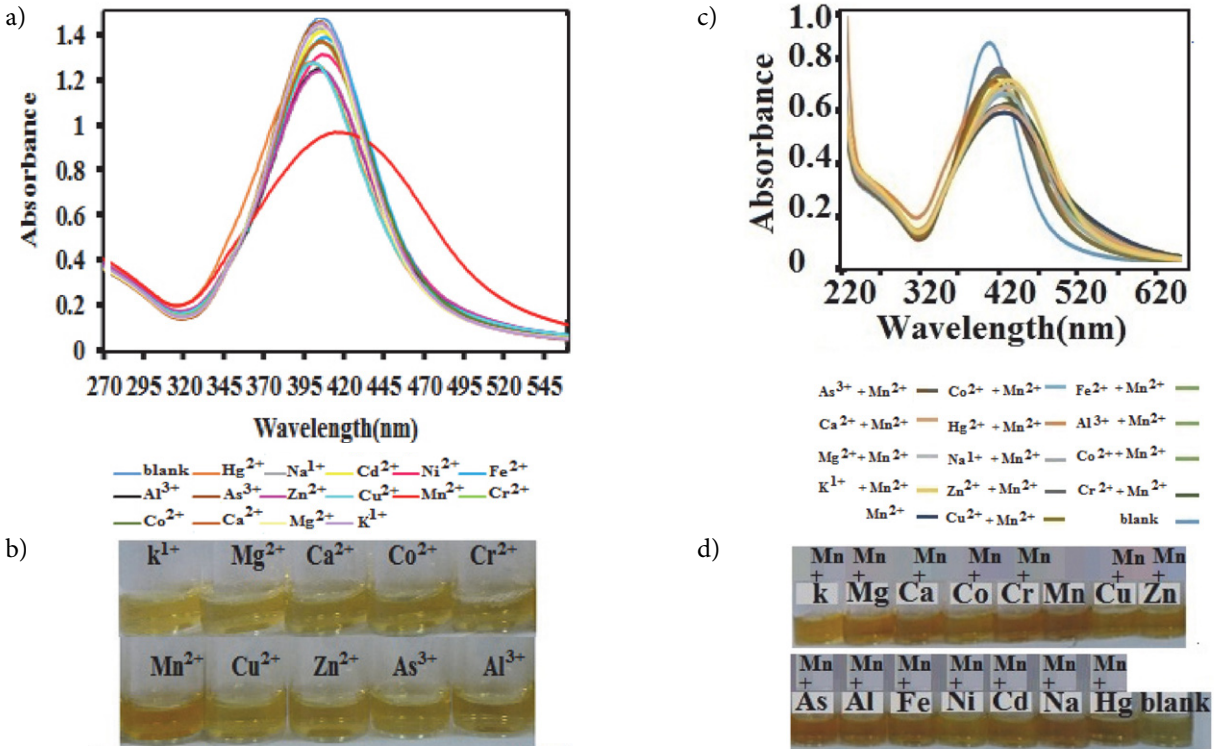

Figure 5. Selectivity of the SDS-AgNPs for Mn^{2+} compared with other ions: (a) UV-vis spectra; (b) photographic images for detecting AgNPs incubated with K^+ (50 μM), Cu^{2+} (50 μM), Hg^{2+} (50 μM), or other ions (50 μM) at pH 7; (c) UV-vis spectra; and (d) Photographic image of detecting SDS-AgNPs incubated with mixture of Mn^{2+} (5 μM) and other ions (5 μM) at pH 7.

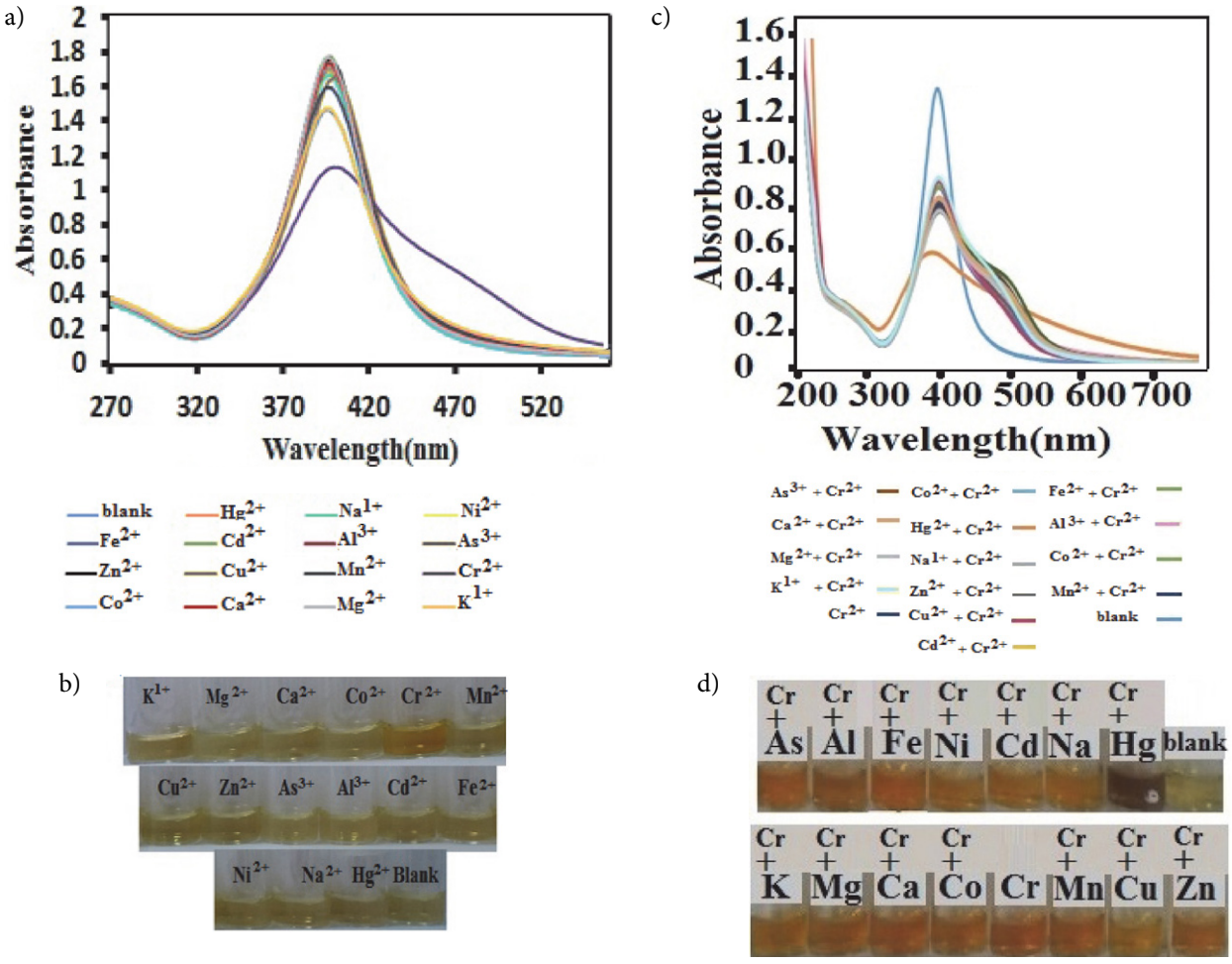

Figure 5. Selectivity of the SDS-AgNPs for Mn^{2+} compared with other ions: (a) UV-vis spectra; (b) photographic images for detecting AgNPs incubated with K^+ (50 μM), Cu^{2+} (50 μM), Hg^{2+} (50 μM), or other ions (50 μM) at pH 7; (c) UV-vis spectra; and (d) Photographic image of detecting SDS-AgNPs incubated with mixture of Mn^{2+} (5 μM) and other ions (5 μM) at pH 7.

significant changes in the SPR absorption intensity and color of solutions, nanoparticles are unstable at pH < 3 and pH > 11. At higher pH values (> 11), SDS-AgNPs aggregate shows a sudden change in the solution color from yellow to orange, a decrease in SPR absorption intensity, and a new peak at 547 nm. According to Mie's theory,[73] due to the exhibition of two bands, SDS-AgNPs may not be spherical and have an anisotropic shape at this range of pH.

From absorption spectra and image of the SDS-CD-AgNPs, it is seen that the particles are stable when pH value changes from 3 to 13. In addition, according to significant changes in the SPR absorption intensity and color of solutions, nanoparticles are unstable at pH < 3.

3. 3. Selectivity Assay of AgNPs

Figures 5 and 6 present that SDS-AgNPs and SDS-CD-AgNPs, when tested against a range of other physiologically and environmentally important cations, have remarkable selectivity for Mn^{2+} and Cr^{2+} ions, respectively. Figures 5(a) and 5(b) show that the other metal ions have no clear effect on the color or UV absorption. Moreover, these Figures show that SDS-AgNPs is efficiently selective for Mn^{2+} ions. Figures 5 (c) and 5 (d) depict the UV-vis spectra of detecting of SDS-AgNPs incubated with a mixture of Mn^{2+} and other metal ions (such as Na^+, K^+, Mg^{2+}, Ca^{2+}, Al^{3+}, As^{3+}, Co^{2+}, Cu^{2+}, Ni^{2+}, Zn^{2+}, Cd^{2+}, Fe^{2+}, Hg^{2+}, and Cr^{2+}) at pH = 7. According to the UV-vis spectra and photographic image, the SDS-AgNPs possess high detection ability and selectivity toward Mn^{2+} in the presence of other cations.

Similarly, Figures 6 (a) and 6 (b) show that SDS-CD-AgNPs have substantial selectivity power for Cr^{2+} ions when tested against a range of other cations. Moreover, these Figures show that the other metal ions have no obvious effect on the color or UV absorption, proving that SDS-CD-AgNPs are sufficiently selective for the Cr^{2+} ions. The UV-vis spectra (Figure 6 (c)) and photographic image (Figure 6 (d)) show the anti-interferential capability of the SDS-CD-AgNPs toward Cr^{2+} in the presence of other competitive ions (e.g., Na^+, K^+, Mg^{2+}, Ca^{2+}, Al^{3+}, As^{3+},

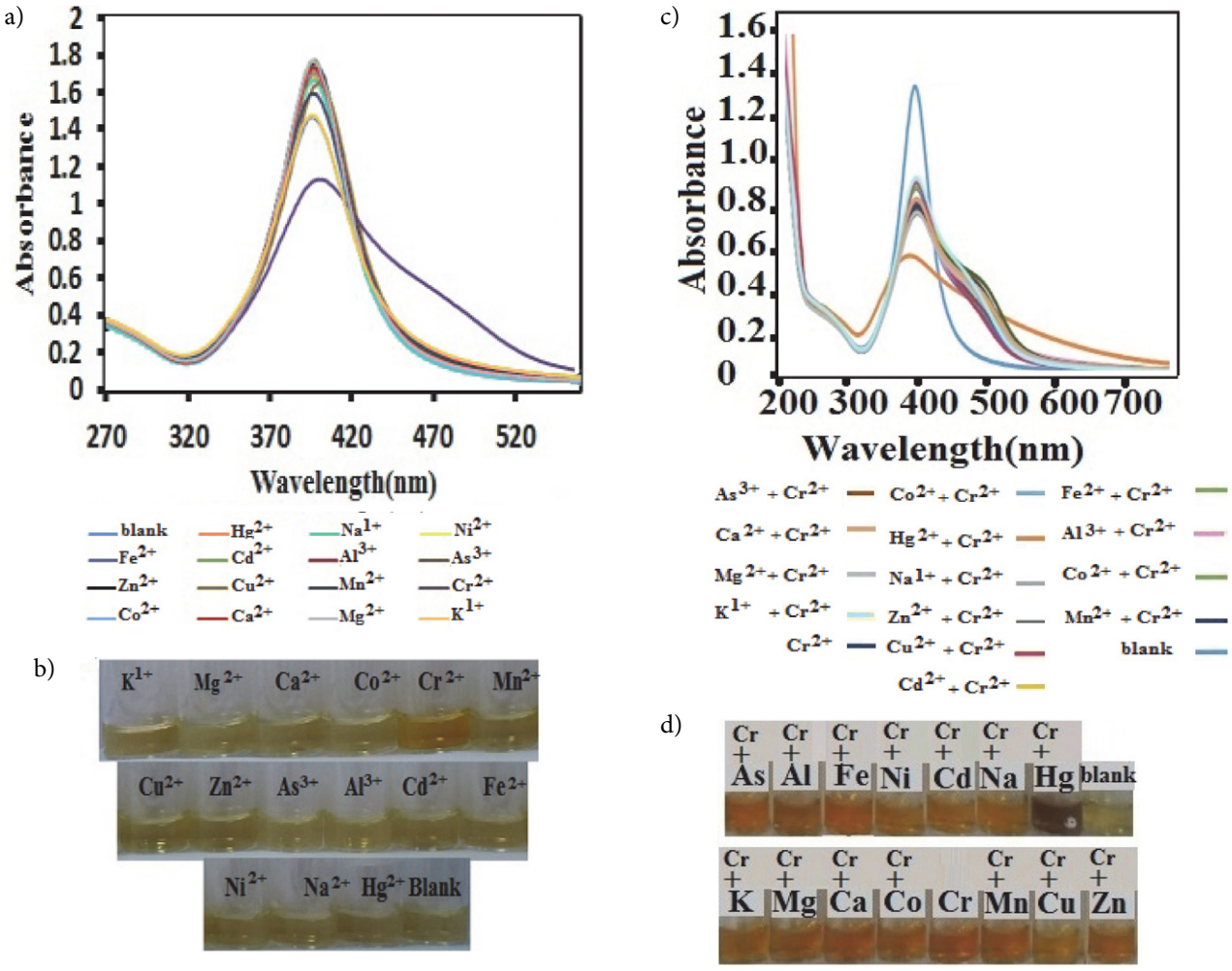

Figure 6. Selectivity of the SDS-CD-AgNPs for Cr^{2+} compared with other ions: (a) UV-vis spectra; (b) photographic images of detecting SDS-CD-AgNPs incubated with K^{+} (5 μM), Cu^{2+} (5 μM), Hg^{2+} (5 μM), or other ions (5 μM) at pH 7; (c) UV-vis spectra; and (d) Photographic image of detecting SDS-CD-AgNPs incubated with the mixture of Cr^{2+} (5 μM) and other ions (5 μM) at pH 7

Co^{2+}, Cu^{2+}, Ni^{2+}, Zn^{2+}, Cd^{2+}, Fe^{2+}, Hg^{2+}, and Mn^{2+} ions) at pH 7. In addition, the results indicate that the solution contacting both Cr^{2+} and Hg^{+} ions changes from yellow to brown. Also, a change in the SPR band was observed (Figure S5). In addition, the absorption ratios of this solution are much lower than the other solutions. These results show that the sensing of Cr^{2+} ions is also possible in the presence of other metal ions and SDS-CD-AgNPs has a good selectivity to Cr^{2+} ions. Furthermore, it is possible to use the SDS-CD-AgNPs solution containing Cr^{2+} ions as an Hg^{2+} sensor. Similar research has been done in this regard.[11, 35]

The sensitivity of SDS-AgNPs toward Mn^{2+} was evaluated by varying the concentration of Mn^{2+} ions (Figure 7). According to this Figure S6, by adding Mn^{2+} ions (1.0 mM to 6.0 μM) to SDS-AgNPs solution, the color of SDS-AgNPs solution changed, which was detected by the naked eye. But, based on the UV-vis spectrum (Figure 7), the changes in the absorption intensity at the maximum wavelength (λ_{410}) showed a linear relationship only in the concentration range from 6.0 μM to 9.0 μM. And in this concentration range the color of the solutions changed from yellow to orange, Figure S6. The LOD and LOQ for Mn^{2+} were 0.02 μM and 0.04 μM, respectively. Similarly, as can be seen from Figure S7, by adding Cr^{2+} ions (1.0 mM to 3.0 μM) to SDS-CD-AgNPs solution, the color of solution changed. But, the changes in the absorption intensity showed a linear relationship with the concentration of Cr^{2+} only in the range from 3.0 μM to 9.0 μM. As Figure 8a Shows, by increasing Cr^{2+} concentration from 3.0 μM to 9.0 μM, the UV-vis absorption peak intensity at 400 nm decreased and the color of the solutions changed from yellow to orange (Figure S7). The LOD and LOQ for Cr^{2+} were 0.01 μM and 0.03 μM, respectively.

3. 4. Real-Time UV-vis Response of AgNP Sensors Toward Desired Ions

Figure S8 shows the changes in the SDS-AgNPs absorbance spectrum after the addition of Mn^{2+} ions. As can be seen, after about 1 min, the colorimetric response of the sensor is observed. Also, after 14 min, the aggre-

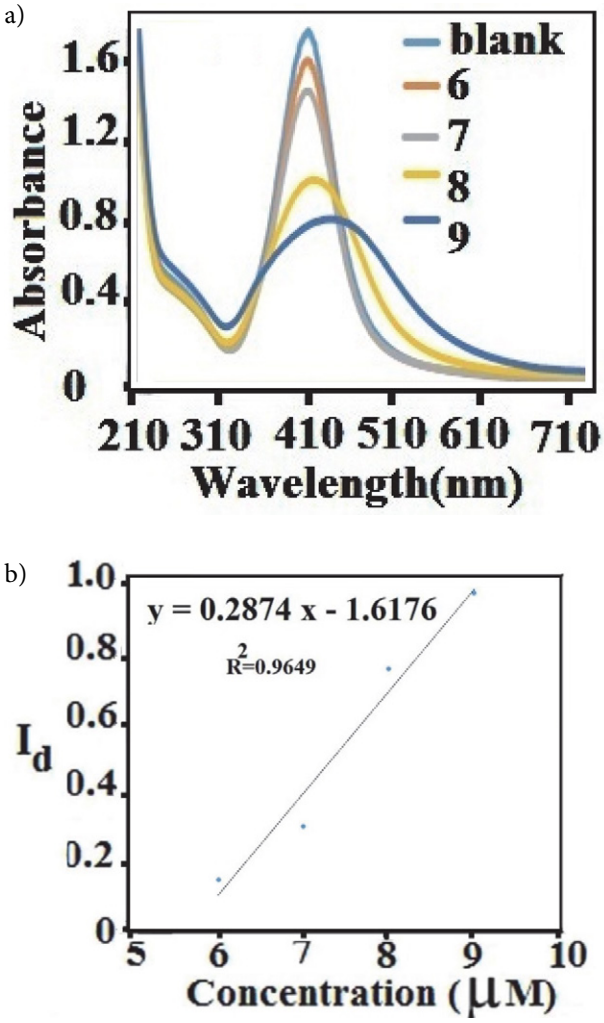

Figure 7. (a) absorption spectral changes observed for SDS-AgNPs after addition of Mn^{2+} ions at a concentration range from 6.0 μM to 9.0 μM and plot of changes in the value of the absorption intensity at the maximum wavelength (λ410) of SDS-AgNPs against Mn^{2+} ion concentration from 6.0 μM to 9.0 μM

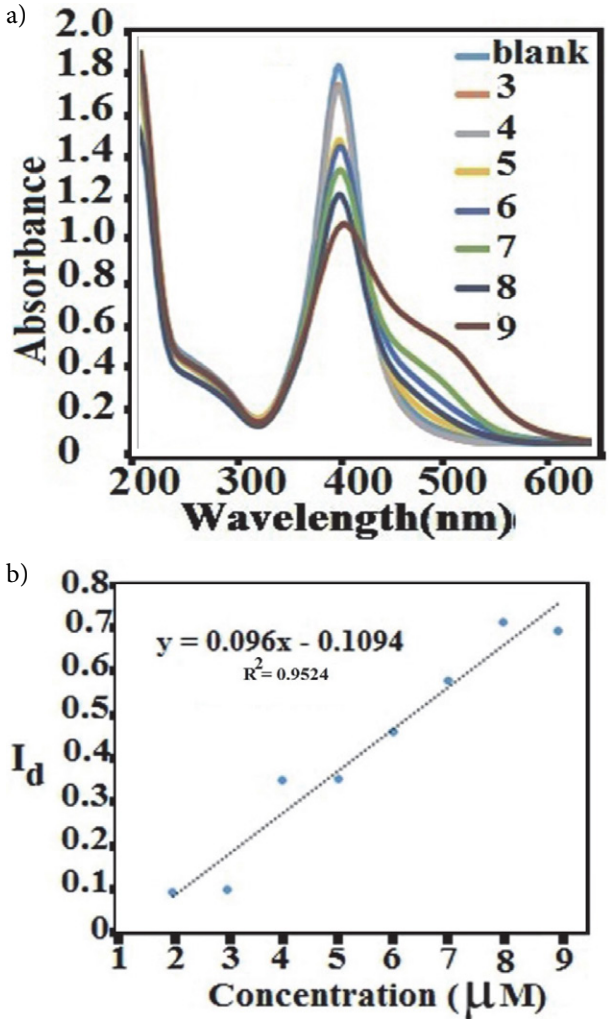

Figure 8. (a) absorption spectral changes observed for SDS-CD-AgNPs after the addition of Cr^{2+} ions at a concentration range from 3 μM to 9.0 μM and (b). The plot of changes in the value of the absorption intensity at the maximum wavelength (λ400) of SDS-CD-AgNPs against Cr^{2+} ions concentration from 3.0 μM to 9.0 μM

gation is completed and there is no change in the absorbance signals.

Similarly, Figure S9 shows that after the addition of Cr^{2+} to the SDS-CD-AgNPs solution, first, there is a decrease in the SPR peak intensity and then it reaches relatively constant values within 4 min.

3. 5. Optimization of the Conditions for the Mn^{2+} or Cr^{2+} Measurement

In the following, the effect of the concentration of the AgNps and pH on the detection of Mn^{2+} or Cr^{2+} ions was investigated.

3. 5. 1. Effect of the Concentration of the AgNps

The effect of the dosage of AgNps on their colorimetric sensing ability is examined as follows: First, different concentrations of AgNPs were prepared with diluting AgNPs solutions in different volumes of deionized water as blank solutions (2:1, 1:1, and 1:2 V:V). Then, different volume ratios of AgNPs solutions to the desired ion solution are prepared (2:1, 1:1, and 1:2).

The absorption spectra and image of Figure 9 reveal that by varying the dosage of AgNps, the colorimetric sensing ability of AgNPs was preserved; however, by increasing the volume ratio of AgNPs solutions to the desired ion solution, a decrease in analytical signal occurs. This reduction could be due to the complexing action of SDS or CD-SDS surface functionality with metal ions (Mn^{2+} or Cr^{2+}), leading to the aggregation of NPs. Also, the Figure shows that by increasing the volume ratio of the AgNPs to the desired ion solution, a higher red shift in the AgNPs SPR band occurred. Since desired ions could complex with surface functionality of several nanoparticles, it can be stated that the presence of more nanoparticles

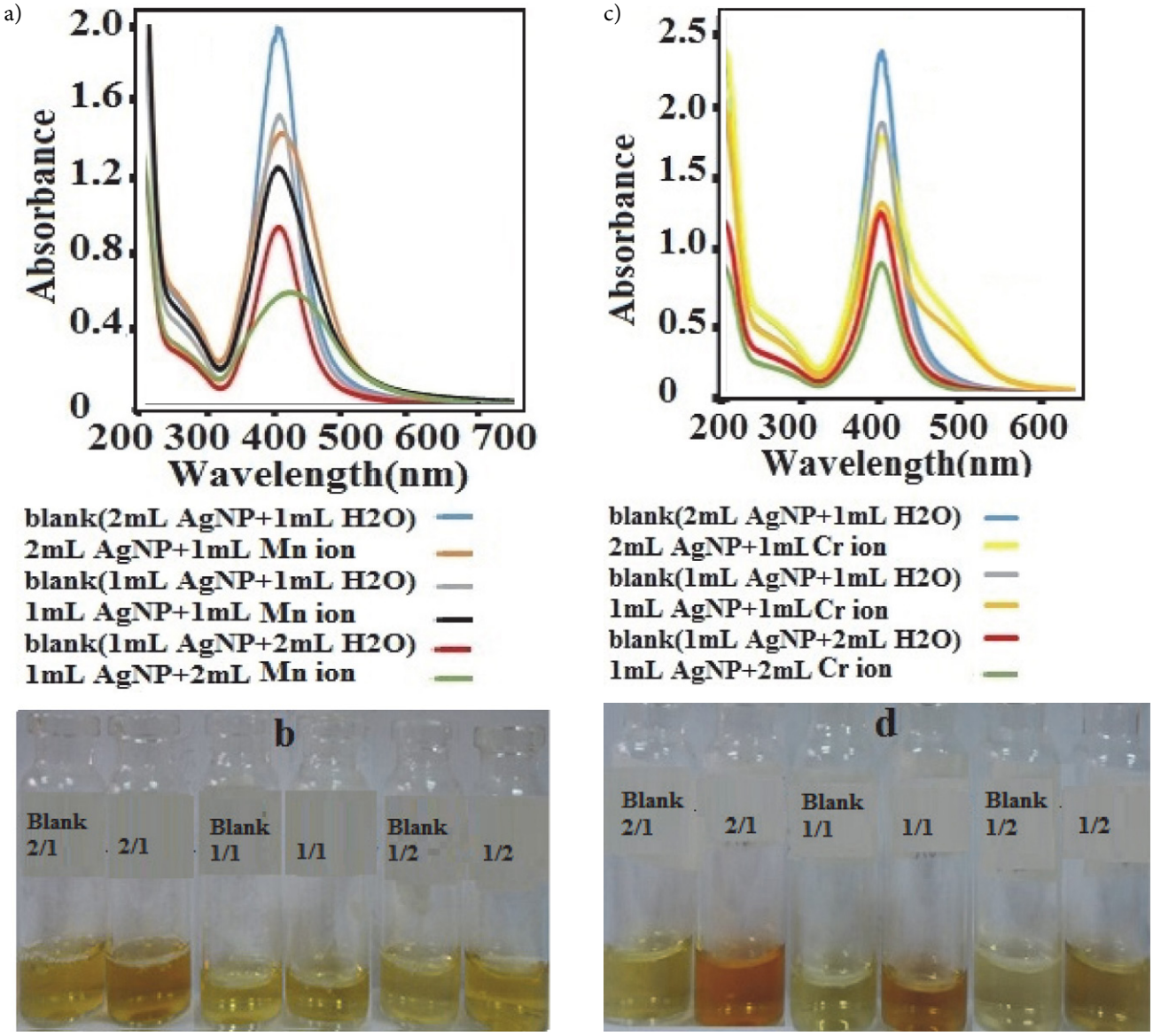

Figure 9. The UV–vis spectra and the photographic images of 2:1, 1:1, and 1:2 volume ratio of (a and b) SDS-AgNPs solutions to Mn^{2+} ions solution and (c and d) SDS-CD-AgNPs solutions to Cr^{2+} ions solution.

around the desired ions in the solution results in agglomeration of more nanoparticle, forming bigger agglomerates, and a higher redshift in the AgNPs SPR band. Thus, the volume ratio of AgNPs to ion solution was selected to be 2:1 with maximal changes in SPR peaks and the color of the solution was selected as the optimal ratio for detecting desired ions by both sensors.

3. 5. 2. Effect of pH on the Detection of Mn^{2+} or Cr^{2+} Ions

The effect of pH on the performance of the sensors was tested as follows. About 1 mL AgNPs solution was mixed with 0.1 ml HCl or NaOH solutions with different concentrations. Next, 1 mL 10 μM Mn^{2+} or Cr^{2+} ions solution was added to the AgNPs solutions. Figure 10 present the effect of pH (1 to 13) on the colorimetric response of the sensors. According to Figure, by adding desired ions to all solutions, a color change and a decrease in the absorbance ratio is clearly observed. These results indicate that both sensors keep their sensing capability at a pH range of 3 to 13. The results show that at the investigated pH range (1–13), pH values of 5 and 11 have more UV-vis intensity changes of the AgNPs solution toward Mn^{2+} detection than the other pHs. Thus, the pHs of 5 and 11 were selected as the best values for detecting manganese ion by SDS-AgNPs in acidic and basic media, receptively. Meanwhile, the pHs of 3 and 9 showed more UV-vis intensity changes toward Cr^{2+} detection than the other pHs. The effect of pH on the colorimetric response of AgNPs can be ascribed to the four factors: (I) AgNPs dissolution (II) forming hydroxide for metal ions, (III) size of AgNPs, and (IV) the effect of electrostatic inter-

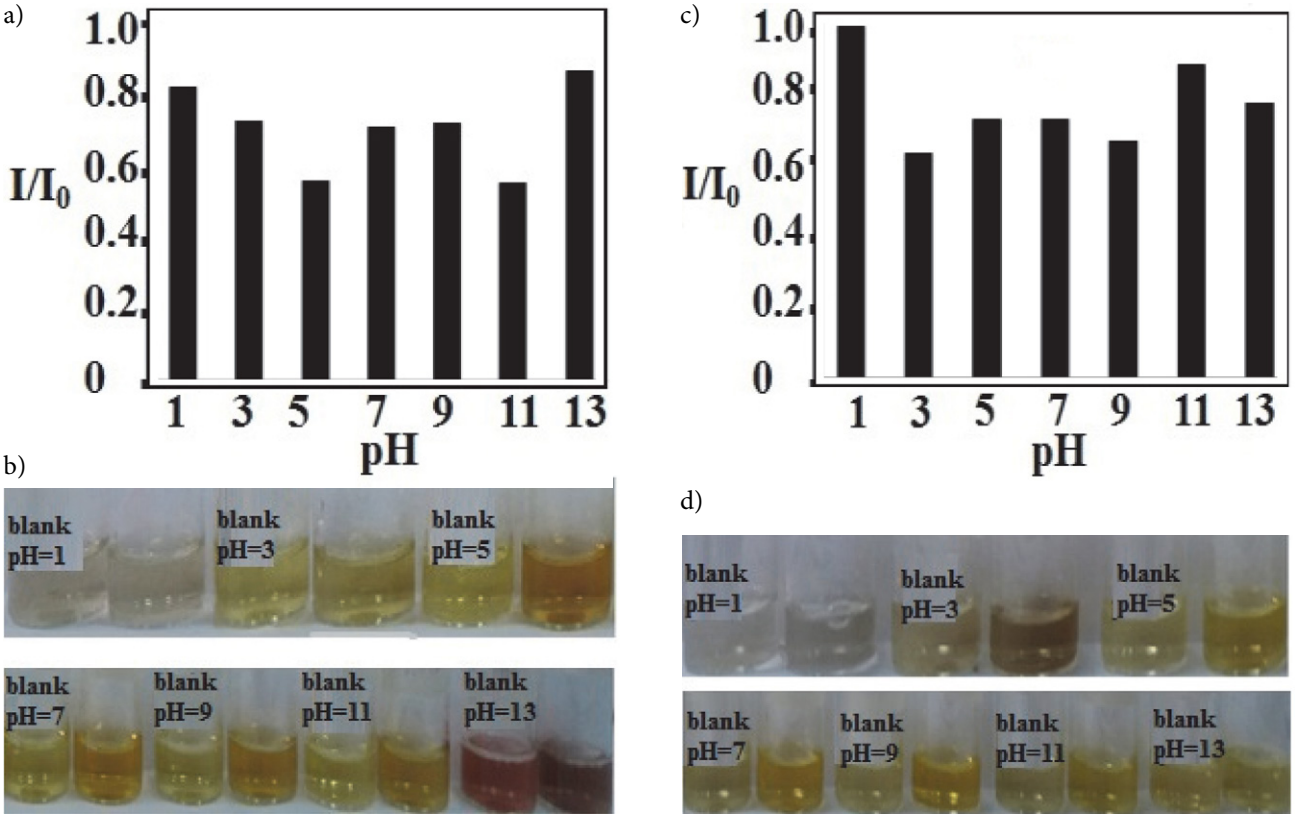

Figure 10. Bar graphs of UV-vis intensity changes and photographic images of (a and b) SDS-CD-AgNPs at different pH levels (c and d) SDS-CD-AgNPs at different pH levels.

action between the negatively charged groups of the surface-bonded SDS or CD and positively charged metal ions.

The results reported in the literature show that particle size has generally an inverse effect on AgNPs dissolution: small AgNPs release more Ag^+ than large ones because smaller particles are energetically unfavorable due to higher surface-to-volume ratio and consequently are more soluble[76]. Based on the TEM results, SDS-AgNPs have a smaller size and a narrower size distribution than SDS-CD-AgNPs. Thus, SDS-CD-AgNPs are more stable than SDS-AgNPs. It was shown at low pH values, AgNPs are dissolved.[76] As can be seen in Figure 10, at pH = 1, both AgNPs are dissolved and no colorimetric response was observed for them. Also, at pH = 3, the SDS-AgNPs have less UV-vis intensity changes toward Mn^{2+} detection than the pH = 5, which could be due to the lower concentration of SDS-AgNPs at pH = 3 than pH = 5. However, at pH = 3, the SDS-CD-AgNPs have the best UV-vis intensity changes toward Cr^{2+} detection, which is due to the larger size of SDS-CD-AgNPs than SDS-AgNPs and their more stability at this pH.

Overall, it can be stated that the performance of SDS-AgNPs and SDS-CD-AgNPs between pH = 5–11 and pH = 3–9 is influenced by two factors, which compete with each other: (I) the size of AgNPs and (II) the electrostatic interaction between the negatively charged groups of AgNPs and positively charged matal ions. Thus, at lower pH, size may control the sensing ability of AgNPs, so that by decreasing pH, the size of particles decreased, as well. And at upper pH, the negative charge of the SDS or CD groups of AgNPs is a more effective factor. So, by increasing pH, SDS surface groups are more deprotonated and, consequently, the electrostatic repulsions between the negatively charged groups increased, leading to an increase in the dispersion of AgNPs. Thus, the desired ions could complex more with surface functionality of nanoparticles than lower pH. Although proper dispersion of nanoparticles enhances the responsiveness of the sensors under alkaline conditions, at pH = 11 for Mn^{2+} and pH = 10 for Cr^{2+}, the sensor performance is reduced due to the formation of manganese hydroxide and chromium hydroxide and, consequently, a decrease in the concentration of Mn^{2+} and Cr^{2+} ions.[50, 52] However, the results indicate that the colorimetric response of SDS-CD-AgNPs at pH = 13 is higher than pH = 11, probably due to the deprotonation of hydroxyl groups of CD bound at the surface of nanoparticles at pH > 12. Therefore, dihydroxylation of OH-groups of cyclodextrin molecules plays a key role in enhancing the formation of Cr^{2+}–CD complex and agglomeration of the nanoparticles.[66]

3. 6. SEM, TEM and DLS Analysis

To explain the mechanism of sensing of the AgNPs to detect desired ions, the nanoparticles were examined

before and after desired exposure using UV-vis, TEM, SEM, and DLS observations. According to the above results, the color of both nanoparticles changes from yellow to orange in the presence of desired ions. The results of TEM, SEM, and DLS for SDS-AgNPs sensor show that SDS-AgNPs are dispersed with small size (Figures 2a, S2a and S3a); but, after adding Mn^{2+} ions, a significant aggregation of nanoparticles is observed (Figures 11a, S 10a and S 11a). Similarly, Figures (2b, S2b and S3b) present the TEM image and SEM and DLS of the SDS-CD-AgNPs sensor. The Figures show the dispersion of the SDS-CD-AgNPs, but adding Cr^{2+} ions resulted in the aggregation of nanoparticles (Figures 11 b, S 10b and S 11b). According to the UV-vis results, with increasing the metal ions concentration (Mn^{2+} or Cr^{2+}), a red shift in the AgNPs SPR band appears. This shift, which could be due to the complexing action of SDS or CD-SDS surface functionality with metal ions (Mn^{2+} or Cr^{2+}), leads to the aggregation of NPs. Thus, for both sensors, the aggregation resulted in reflecting the ion-induced aggregation of the functional AgNPs. As mentioned, according to the information obtained from previous studies,[68,77] it is very likely that the SDS was adsorbed on the surface of nanoparticles through hydrophobic bonding with a tail surface/headwater orientation. The high selectivity of the SDS-AgNP toward Mn^{2+} can be attributed to two phenomena: (I) the cooperative effect of electrostatic interaction between the negatively charged SO^{4-} groups of SDS and positively charged Mn^{2+} ions and (II) the complexation of Mn^{2+} ions as hard acids with oxygen donors of SDS. Accordingly, the SDS-AgNPs tend to come closer, which decreases the interparticle distance and makes them aggregated. According to the lectures,[78, 79] cyclodextrin stabilizes the surface of AgNPs through chemisorption of hydroxyl groups and the hydrophobic-hydrophobic interactions. Thus, the CD has been applied as both stabilizer and surface functionalizing agents for AgNPs synthesis. Furthermore, as mentioned earlier, in the SDS-CD-AgNPs, the AgNPs are capped by the host-guest inclusion of SDS-CD. According to the obtained results, SDS-AgNPs do not respond to the Cr^{2+} ions. In comparison, the SDS-CD-AgNPs demonstrates sensitive and selective colorimetric detection of Cr^{2+} ions. Probably, Cr^{2+} ion as a harder acid than Mn^{2+} ion in addition to bind sulfate groups and oxygen donors of SDS, has tendency to bind ether and hydroxyl groups of cyclodextrin. Thus, selectivity of the SDS-CD-AgNPs toward Cr^{2+} can be ascribed to the three facators: (I) The cooperative effect of electrostatic interaction between the negatively charged SO_4^- groups of SDS and positively charged Cr^{2+} ions; (II) The complexation of Cr^{2+} ions as hard acids with oxygen donors of SDS; and (III) The complexation of Cr^{2+} ions as hard acids with ether and hydroxyl groups of cyclodextrin as hard base. Owning to these reasons, the SDS-CD-AgNPs tend to keep closer, decreasing the interparticle distance and gets aggregated. Based on TEM results, the aggregates of the SDS-CD-AgNPs in the presence of Cr^{2+} ions are larger than those of the SDS-AgNPs in the presence of Mn^{2+} ions. This can be attributed that the SDS-CD-AgNPs are more agglomerate than SDS-AgNps, Figure 2. In addition, as mentioned, the interaction between SDS and CD surface groups with desired ions are different.

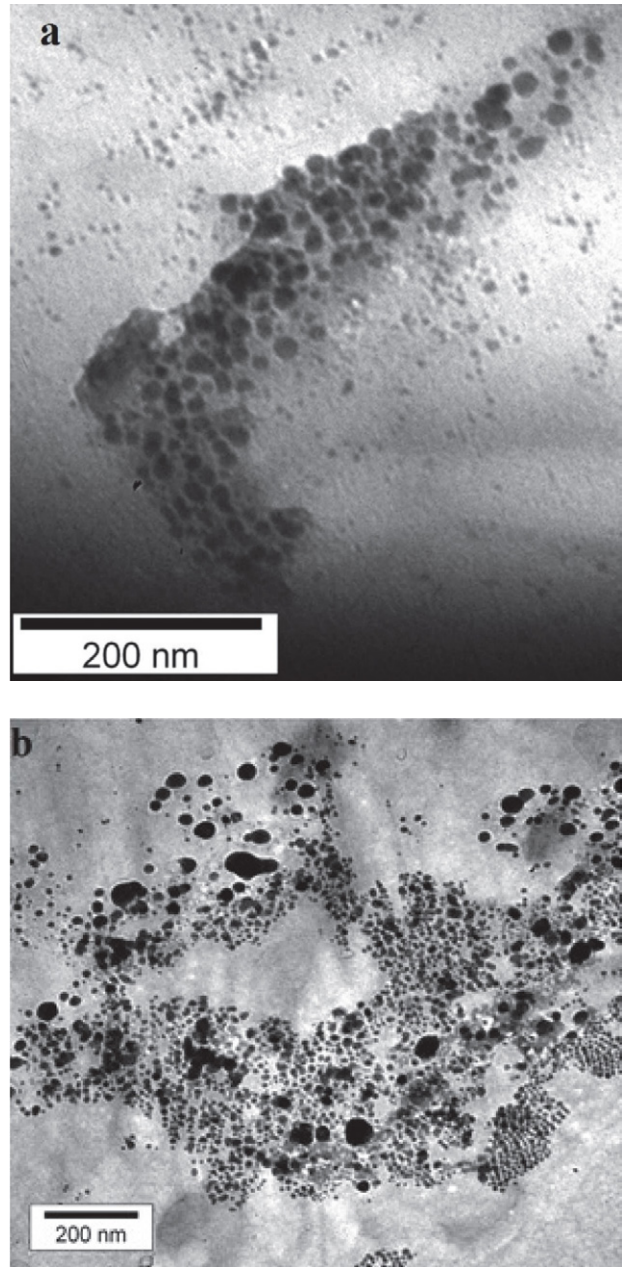

Figure 11. TEM images (a) of SDS-AgNPs after the addition of 0.5 μM of Mn^{2+} ions (b) of SDS-CD-AgNPs after the addition of 0.5 μM of Cr^{2+} ions.

Table 1 summarizes information of various Mn^{2+} detection methods based on AgNPs as a colorimetric sensor. In contrast to some studies [49,80,81] reported in the table, SDS-AgNPs have much lower detection level for Mn^{2+} ions. As shown in Table 1, although the sensing ability of sensors reported in this Table is suitable, compared to our

Table 1. Comparison of different methods using AgNPs as a colorimetric sensor for Mn^{2+} detection.

No	Time of preparation	Capping agents	pH range	Detection time (min)	Selectivity	LOD	Ref
1	2.5 h	B-cyclodextrin and Adamantine	–	5	Selective μM	0.5	[80]
2	24.5 h	Sodium pyrophosphate and hydroxyl propyl methyl cellulose	12	10	selective	2 nM	[50]
3	5 min	L-tyrosine	7–12	–	Responsive for Hd^{2+} and Mn^{2+}	16 nM	[52]
4	1.20 h with sonicate	5-sulfoanthranilic acid di thiocarbamate	2–12	1	Responsive to Cd^{2+} and Mn^{2+}	3 nM	[51]
6	1 h	Pyrophosphate	More than pH 9.0	–	Selective	0.03 μM	[49]
7	0.5 h	l-arginine	9.4	40	Selective	20 nM	[16]
8	1 h	alginate	10	30	Selective	2 μM	[53]
9	5 min	tripolyphosphate	Lower than 11.5		Selective	0.1 μM,	[81]
10	2 h	Sodium dodecyl sulfonate	3–11	14	Selective	0.02 μM	This work

Table 2. Comparison of colorimetric sensing probe for Cr^{2+}detection.

No	Time of preparation (hour)	Capping agents	pH range	Detection time	Selectivity	LOD (μM)	Ref
1	75	Rhodamine B, Umbelliferone	–	–	Selective	64	[58]
2	2	Sodium dodecyl sulfonate and β-cyclodextrin	3–11	4 min	Selective	0.01	This work

study, each of them has some limitations. For example, colorimetric sensors reported by Wu et al.[50] Chen et al.[49], He et al.[16] and Badri et al.[53] had a detection limitation with respect to pH conditions for Mn^{2+} ions. Compared with these reports for the colorimetric detection of Mn^{2+}, our method provided a good detection performance of Mn^{2+} for the pH range of 1 to 13. Moreover, according to Table 1, the sensors reported by Annadhasan et al.[52] and Vaibhavkumar et al.[51] suffered from selectivity limitations of detecting Mn^{2+} ions. Compared with these works, the sensors in our work are selective only for Mn^{2+} detection. In some studies reported by Wu et al.[50] and Vaibhavkumar et al,[51] the AgNPs sensor preparation process is complicated. Our approach to synthesize SDS-AgNPs is not time-consuming and costly. Table 2 summarizes information of Cr^{2+} detection method based on the colorimetric sensing probe. According to Table 2, our method provided a better sensing ability for detecting Cr^{2+} for the pH range of 1 to 13 and a good response rate. Compared to Rull-Barrull's work, our sensor has a higher sensitivity. As well as, in Rull-Barrull's study, the AgNPs sensor preparation process is complicated.[58]

4. Conclusion

In summary, two types of stable silver nanoparticles (AgNPs) were synthesized with SDS and a combination of SDS and CD, which were successfully utilized as a colorimetric sensor for Mn^{2+} and Cr^{2+} ions at ppm level, respectively. Upon adding desired ions, both AgNPs solutions changed from yellow to orange, which was detected by the naked eye and UV-vis spectroscopy. Indeed, the desired ions can be detected rapidly based on the color change of the system, due to the aggregation of Ag nanoparticles by adsorbing metal ions on their surface.

5. References

1. J. L. Aschner and M. Aschner, *Mol Aspects med* **2005**, *26*, 353–362. **DOI:**10.1016/j.mam.2005.07.003
2. R. T. Achmad and E. I. Auerkari, *Annu Rev Plant BioL.* **2017**, 1–8. **DOI:**10.9734/ARRB/2017/33462
3. M. Faisal and S. Hasnain, *J. Pharmacol. Toxicol* **2006**, *1*, 248–258.
4. S. L. O'Neal and W. Zheng, *Current environmental health reports* **2015**, *2*, 315–328. **DOI:**10.1007/s40572-015-0056-x
5. S. H. Frisbie, E. J. Mitchell, H. Dustin, D. M. Maynard and B. Sarkar, *Environ Health Perspect.* **2012**, *120*, 775–778. **DOI:**10.1289/ehp.1104693
6. M. Deveau, J Toxicol Environ *Health. Part A* **2010**, *73*, 235–241. **DOI:**10.1080/15287390903340880
7. J. Mao, Q. He and W. Liu, *Anal Bioanal Chem* **2010**, *396*, 1197–1203. **DOI:**10.1007/s00216-009-3161-6

8. K. Dutta, R. C. Deka and D. K. Das, *J. Fluoresc.* **2013**, *23*, 1173–1178. **DOI:**10.1007/s10895-013-1248-0
9. U. Divrikli, M. Soylak and L. Elci, *Environ Monit Assess.* **2008**, *138*, 167–172. **DOI:**10.1007/s10661-007-9754-7
10. V. Doroschuk, S. Lelyushok, V. Ishchenko and S. Kulichenko, *Talanta* **2004**, *64*, 853–856. **DOI:**10.1016/j.talanta.2004.03.056
11. W. Zhou, B.-C. Yin and B.-C. Ye, *Biosens Bioelectron* **2017**, *87*, 187–194.
12. A. Ramesh, B. A. Devi, H. Hasegsawa, T. Maki and K. Ueda, *MicrocheM J.* **2007**, *86*, 124–130. **DOI:**10.1016/j.microc.2007.01.002
13. A. Milne, W. Landing, M. Bizimis and P. Morton, *Anal. Chim. Acta* **2010**, *665*, 200–207. **DOI:**10.1016/j.aca.2010.03.027
14. H. Gürleyük and D. Wallschläger, *J. Anal. At. Spectrom.* **2001**, *16*, 926–930. **DOI:**10.1039/B102740A
15. E. Grygo-Szymanko, A. Tobiasz, N. Miliszkiewicz, D. Dudek-Adamska and S. Walas, *Analytical Letters* **2017**, *50*, 2147–2160. **DOI:**10.1080/00032719.2016.1267185
16. Y. He and X. Zhang, *Sensors and Actuators B: Chemical* **2016**, *222*, 320–324. **DOI:**10.1016/j.snb.2015.08.089
17. Y.-X. Qi, Z.-b. Qu, Q.-X. Wang, M. Zhang and G. Shi, *Anal. Chim. Acta* **2017**, *980*, 65–71. **DOI:**10.1016/j.aca.2017.05.018
18. Y. Zhao and Z. Zhong, *J. Am.Chem. Soc* **2006**, *128*, 9988–9989. **DOI:**10.1021/ja062001i
19. X. Liu, Y. Tang, L. Wang, J. Zhang, S. Song, C. Fan and S. Wang, *Advanced Materials* **2007**, *19*, 1471–1474. **DOI:**10.1002/adma.200602578
20. I.-B. Kim and U. H. Bunz, *J. Am.Chem. Soc* **2006**, *128*, 2818–2819. **DOI:**10.1021/ja058431a
21. X. Xu, J. Wang, K. Jiao and X. Yang, *Biosensors and Bioelectronics* **2009**, *24*, 3153–3158. **DOI:**10.1016/j.bios.2009.03.025
22. D. Zhang, M. Deng, L. Xu, Y. Zhou, J. Yuwen and X. Zhou, *Chemistry–A European Journal* **2009**, *15*, 8117–8120. **DOI:**10.1002/chem.200901268
23. M. Hollenstein, C. Hipolito, C. Lam, D. Dietrich and D. M. Perrin, *Angewandte Chemie International Edition* **2008**, *47*, 4346–4350. **DOI:**10.1002/anie.200800960
24. M. Rex, F. E. Hernandez and A. D. Campiglia, *Anal Lett.* **2006**, *78*, 445–451. **DOI:**10.1021/ac051166r
25. Y.-R. Kim, R. K. Mahajan, J. S. Kim and H. Kim, *ACS Appl Mater Inter.* **2009**, *2*, 292–295. **DOI:**10.1021/am9006963
26. P. Vasileva, T. Alexandrova and I. Karadjova, *J Chem* **2017**, *2017*. **DOI:**10.1155/2017/6897960
27. S. S. J. Xavier, G. Siva, J. Annaraj, A. R. Kim and D. J. Yoo, *Sens Actuators B Chem* **2018**, *259*, 1133–1143. **DOI:**10.1016/j.snb.2017.12.046
28. K. Ramachandran and K. J. Babu, *Sci Rep* **2016**, *6*, 36583. **DOI:**10.1038/srep36583
29. K. J. Babu, N. Senthilkumar and A. R. Kim, *Sens Actuators B Chem* **2017**, *241*, 541–551. **DOI:**10.1016/j.snb.2016.10.069
30. P. Wuamprakhon, A. Krittayavathananon, N. Ma, N. Phattharasupakun, T. Maihom, J. Limtrakul and M. Sawangphruk, *J Electroanal Chem.* **2018**, *808*, 124–132. **DOI:**10.1016/j.jelechem.2017.12.003
31. K. J. Babu, D. J. Yoo and A. R. Kim, *RSC Adv.* **2015**, *5*, 41457–41467. **DOI:**10.1039/C5RA03305E
32. K. J. Babu, T. Raj Kumar, D. J. Yoo, S.-M. Phang and G. Gnana kumar, *ACS Sustain Chem Eng.* **2018**, *6*, 16982–16989. **DOI:**10.1021/acssuschemeng.8b04340
33. C. Burda, X. Chen, R. Narayanan and M. A. El-Sayed, *Chem Rev.* **2005**, *105*, 1025–1102. **DOI:**10.1021/cr030063a
34. R. Shukla, V. Bansal, M. Chaudhary, A. Basu, R. R. Bhonde and M. Sastry, *Langmuir* **2005**, *21*, 10644–10654. **DOI:**10.1021/la0513712
35. V. V. Kumar and S. P. Anthony, *Sens Actuators B Chem* **2014**, *191*, 31–36. **DOI:**10.1016/j.snb.2013.09.089
36. W. Leesutthiphonchai, W. Dungchai, W. Siangproh, N. Ngamrojnavanich and O. Chailapakul, *Talanta* **2011**, *85*, 870–876. **DOI:**10.1016/j.talanta.2011.04.041
37. T. Kim, C.-H. Lee, S.-W. Joo and K. Lee, *J colloid interf sci* **2008**, *318*, 238–243. **DOI:**10.1016/j.jcis.2007.10.029
38. L. Wei, Z. Yuping, C. Chengxing, C. Wentao, L. Runqiang and Q. Lingbo: 2011 Third International Conference on Measuring Technology and Mechatronics Automation, IEEE, 2011, pp. 1013–1016.
39. K. Aslan, J. R. Lakowicz and C. D. Geddes, *Anal. Biochem.* **2004**, *330*, 145–155. **DOI:**10.1016/j.ab.2004.03.032
40. B. Paul and A. Tiwari, *IOSR J. Environ. Sci. Toxicol. Food Technol.(Iosr-Jestft)* **2015**, *1*, 1–7.
41. E. Priyadarshini and N. Pradhan, *Sens Actuators B Chem* **2017**, *238*, 888–902. **DOI:**10.1016/j.snb.2016.06.081
42. B. A. Makwana, D. J. Vyas, K. D. Bhatt, S. Darji and V. K. Jain, *Appl. Nanosci.* **2016**, *6*, 555–566. **DOI:**10.1007/s13204-015-0459-x
43. H. Li, Z. Cui and C. Han, *Sens Actuators B Chem* **2009**, *143*, 87–92. **DOI:**10.1016/j.snb.2009.09.013
44. R. Rajamanikandan and M. Ilanchelian, *Mater Today Commun.* **2018**, *15*, 61–69. **DOI:**10.1016/j.mtcomm.2018.02.024
45. H. K. Sung, S. Y. Oh, C. Park and Y. Kim, *Langmuir* **2013**, *29*, 8978–8982. **DOI:**10.1021/la401408f
46. Y.-r. Ma, H.-y. Niu and Y.-q. Cai, *Chem Comm* **2011**, *47*, 12643–12645. **DOI:**10.1039/c1cc15048k
47. C. J. Kirubaharan, D. Kalpana, Y. S. Lee, A. Kim, D. J. Yoo, K. S. Nahm and G. G. Kumar, *Ind Eng Chem Res.* **2012**, *51*, 7441–7446. **DOI:**10.1021/ie3003232
48. X. Gao, Y. Lu, S. He, X. Li and W. Chen, *Anal. Chim. Acta* **2015**, *879*, 118–125. **DOI:**10.1016/j.aca.2015.04.002
49. L. Chen, Y. Ye, H. Tan and Y. Wang, *Colloid Surface A.* **2015**, *478*, 1–6.
50. G. Wu, C. Dong, Y. Li, Z. Wang, Y. Gao, Z. Shen and A. Wu, *RSC Adv.* **2015**, *5*, 20595–20602. **DOI:**10.1039/C5RA00001G
51. V. N. Mehta, J. V. Rohit and S. K. Kailasa, *New J Chem.* **2016**, *40*, 4566–4574. **DOI:**10.1039/C5NJ03454J

52. M. Annadhasan, T. Muthukumarasamyvel, V. Sankar Babu and N. Rajendiran, *ACS Sustain Chem Eng.* **2014**, *2*, 887–896. **DOI:**10.1021/sc400500z
53. K. B. Narayanan and S. S. Han, *Res Chem Intermediat.* **2017**, *43*, 5665–5674. **DOI:**10.1007/s11164-017-2954-z
54. A. Ravindran, M. Elavarasi, T. Prathna, A. M. Raichur, N. Chandrasekaran and A. Mukherjee, *Sensor Actuat B-Chem.* **2012**, *166*, 365–371. **DOI:**10.1016/j.snb.2012.02.073
55. A. Ravindran, V. Mani, N. Chandrasekaran and A. Mukherjee, *Talanta* **2011**, *85*, 533–540. **DOI:**10.1016/j.talanta.2011.04.031
56. M. Elavarasi, A. Rajeshwari, S. A. Alex, D. N. Kumar, N. Chandrasekaran and A. Mukherjee, *Anal Methods.* **2014**, *6*, 5161–5167. **DOI:**10.1039/c4ay00877d
57. R. P. Modi, V. N. Mehta and S. K. Kailasa, *Sensor Actuat B-Chem.* **2014**, *195*, 562–571. **DOI:**10.1016/j.snb.2014.01.059
58. J. Rull-Barrull, M. d'Halluin, E. Le Grognec and F.-X. Felpin, *Tetrahedron Lett.* **2017**, *58*, 505–508. **DOI:**10.1016/j.tetlet.2016.12.038
59. J. K. Patra and K.-H. Baek, *J. Nanomater.* **2014**, *2014*, 219. **DOI:**10.1155/2014/417305
60. S. Agnihotri, S. Mukherji and S. Mukherji, *RSC Adv.* **2014**, *4*, 3974–3983. **DOI:**10.1039/C3RA44507K
61. G. Mie, *Ann. Phys* **1908**, *25*, 377–442. **DOI:**10.1002/andp.19083300302
62. H. Wang, Y. Wang, J. Jin and R. Yang, *Anal. Chem.* **2008**, *80*, 9021–9028. **DOI:**10.1021/ac801382k
63. E.-J. Bae, H.-J. Park, J.-S. Park, J.-Y. Yoon, Y.-H. Kim, K.-H. Choi and J.-H. Yi, *Bull. Korean Chem. Soc.* **2011**, *32*, 613–619. **DOI:**10.5012/bkcs.2011.32.2.613
64. H. Zhang and C. Zhang, *J. Mater. Environ. Sci.* **2014**, *5*, 231–236.
65. Z. Li, H. Li, C. Wang, J. Xu, V. Singh, D. Chen and J. Zhang, *Acta Pharm. Sin. B.* **2016**, *6*, 344–351. **DOI:**10.1016/j.apsb.2016.03.003
66. E. Gaidamauskas, E. Norkus, E. Butkus, D. C. Crans and G. Grincienė, *Carbohydr. Res.* **2009**, *344*, 250–254. **DOI:**10.1016/j.carres.2008.10.025
67. I. Niskanen, V. Forsberg, D. Zakrisson, S. Reza, M. Hummelgård, B. Andres, I. Fedorov, T. Suopajärvi, H. Liimatainen and G. Thungström, *Chem. Eng. Sci.* **2019**, *201*, 222–229. **DOI:**10.1016/j.ces.2019.02.020
68. S. A. Ghoto, M. Y. Khuhawar and T. M. Jahangir, *Anal Sci* **2019**, 18P417.
69. C. Yuan, B. Liu and H. Liu, *Carbohydr. Polym.* **2015**, *118*, 36–40. **DOI:**10.1016/j.carbpol.2014.10.070
70. R. Azimpanah, Z. Solati and M. Hashemi, *Iet Nanobiotechnol.* **2018**, *12*, 673–677. **DOI:**10.1049/iet-nbt.2017.0236
71. A. Alam, A. Ravindran, P. Chandran and S. S. Khan, *Spectrochim Acta A Mol Biomol* Spectrosc. **2015**, *137*, 503–508. **DOI:**10.1016/j.saa.2014.09.004
72. B. Qiao, Y. Liang, T.-J. Wang and Y. Jiang, *Appl Surf Sci.* **2016**, *364*, 103–109. **DOI:**10.1016/j.apsusc.2015.12.116
73. V. Amendola, S. Polizzi and M. Meneghetti, *Langmuir* **2007**, *23*, 6766–6770. **DOI:**10.1021/la0637061
74. D. V. Leff, P. C. Ohara, J. R. Heath and W. M. Gelbart, *Am. J. Phys. Chem.* **1995**, *99*, 7036–7041. **DOI:**10.1021/j100018a041
75. G. Mie, *Ann. Phys* **1908**, *25*, 377–442. **DOI:**10.1002/andp.19083300302
76. B. Molleman and T. Hiemstra, *Environ. Sci. Nano* **2017**, *4*, 1314–1327. **DOI:**10.1039/C6EN00564K
77. A. López-Miranda, A. López-Valdivieso and G. Viramontes-Gamboa, *J Nanopart Res.* **2012**, *14*, 1101. **DOI:**10.1007/s11051-012-1101-4
78. S. S. J. Xavier, C. Karthikeyan, A. R. Kim and D. J. Yoo, *Anal Methods.* **2014**, *6*, 8165–8172. **DOI:**10.1039/C4AY01183J
79. Q. Ma, J. Song, S. Zhang, M. Wang, Y. Guo and C. Dong, *Colloids Surf B Biointerfaces* **2016**, *148*, 66–72. **DOI:**10.1016/j.colsurfb.2016.08.040
80. R. Hu, L. Zhang and H. Li, *New J Chem* **2014**, *38*, 2237–2240. **DOI:**10.1039/C3NJ01593A
81. Y.-X. Gao, J.-W. Xin, Z.-Y. Shen, W. Pan, X. Li and A.-G. Wu, *Sens Actuators B Chem* **2013**, *181*, 288–293. **DOI:**10.1016/j.snb.2013.01.079

Povzetek

V študiji smo razvili preprosto, hitro, občutljivo, selektivno in poceni kolorimetrično metodo za določanje magnezijevih (Mn^{2+}) in kromovih (Cr^{2+}) ionov v vodnih raztopinah. Natrijev dodecil sulfat (SDS) in β-ciklodekstrin (CD) sta bila uporabljena kot stabilizatorja in površinsko aktivni snovi za sintezo srebrovih nanodelcev (AgNPs). Sintetizirane AgNPs smo okarakterizirali s FT-IR spektroskopijo, UV-vis spektroskopijo, vrstično elektronsko mikroskopijo (SEM) in dinamičnim sipanjem svetlobe (DLS). Preučili smo tudi vpliv pH vrednosti na stabilnost AgNPs. Srebrovi nanodelci modificirani z SDS (SDS-AgNPs) in z SDS ter β-ciklodekstrinom (SDS-CD-AgNPs) izkazujejo občutljivost in so uporabni za kolorimetrično detekcijo Mn^{2+} in Cr^{2+} ionov v ppm koncentracijah. SDS-AgNPs in SDS-CD-AgNPs povzročijo barvno spremembo vidno s prostim očesom iz rumene v oranžno po dodatku Mn^{2+} in Cr^{2+} ionov medtem ko ostali ioni tega ne povzročijo. Rezultati SEM in DLS kažejo, da dodatek Mn^{2+} ali Cr^{2+} ionov povzroči agregacijo delcev. Tekom študije smo tako uspeli sintetizirati AgNPs, SDS-AgNPs in SDS-CD-AgNPs, ki lahko služijo kot preprost, hiter, občutljiv in selektivni kolorimetrični senzor z znatnim potencialom za hitro detekcijo Mn^{2+} in Cr^{2+} ionov na terenu.